Appendix F: Modification of GRW Tanker Proprietary Finite Element model

1 Overview

TWI has conducted finite element analysis (FEA) of a fuel-tanker, J3857, in order to perform fracture and fatigue engineering critical assessment calculations using BS 7910. The FEA model was originally produced by GRW (2013). TWI has modified the geometry, meshing strategy and stress extraction method in order to more accurately predict the stresses in the tanker. Hot spot stresses were extracted from the model for each tanker band weld for three different load cases: vertical, lateral and longitudinal unit load accelerations. The stresses predicted from the FEA model were then scaled by real acceleration measurements in order to produce stress-time histories for use in a fatigue analysis.

2 Geometry

The J3857 tanker geometry was modelled in detail (see Figure 1), including the tanker shell, baffles and bulkheads, extrusion bands, valance, undercarriage and suspension system. The tanker was predominantly modelled with shells, which is appropriate for a thin-walled vessel. The suspension system was modelled using a combination of beams, linear springs, hinges, ball joints and bushings.

Cracks have been observed in the tankers between the extrusion bands and the tanker shell. Therefore, this is the most critical part of the geometry, where stresses would be extracted from the model. This means that any key features of the geometry around these locations that may affect the stresses should be included in the model. On inspection of the geometry of the GRW model compared to engineering drawings (GRW, 2008 (1) and (2)), it appears that some details were omitted from the model which may impact the stresses in those areas. In particular, a bulkhead (solid plate) in the model should in fact be a baffle (central hole in plate) (see Figure 2). Also, the modelling of the baffles did not include a small hole at the bottom of the baffle (Figure 3), which would act as a stress concentrating feature at this location. Stiffeners were also not included on the LL box, which may affect the stresses in the shell near this location. These features have all been included in the TWI model (see Figure 4), using tie constraints between the baffles and extrusion bands to simplify the meshing strategy.

The modelling methodology used for the extrusion band geometry was also changed from the original GRW model in order to make it more representative of the real tanker geometry. This is illustrated in Figure 5, where the tanker band extends from A to D, with welds positioned at B and C. The GRW model used a constant section thickness of 15mm for section A to C, and a constant section thickness of 5mm for section A to D. This underestimates the bending stiffness of the component, because the areas of the band from A to B and from C to D are not included in the model. TWI have modelled the tanker band with 15mm thickness from B to D, but this shell is only connected to the tanker shell at locations A and C (using Abaqus TIE constraints). This means the model is representing the bending stiffness of the bands more realistically, whilst keeping the weld toes in the correct position.

3 Mesh

The tanker was meshed with 1.8 million quadratic quadrilateral elements (type S8R in Abaqus), 672,000 linear quadrilateral elements (type S4R in Abaqus), 23,000 linear triangular elements (type S3 in Abaqus) and 2,478 linear line elements (type B31 in Abaqus) for the suspension and bolts. The GRW was originally meshed entirely with linear elements, which may not predict stresses accurately enough in a static 1g analysis without significant mesh refinement. Hence, the TWI model used quadratic elements in the shell and tanker bands, where the stresses would be extracted from the model. The local mesh size at the intersection between the extrusion bands and the shell tanker was 5mm, which is equal to the tanker shell thickness. Elements of the order of the shell thickness are recommended for accurate stress prediction. A global mesh size of 25mm was used far away from the areas of interest, with a smooth transition in element size being used, as shown in Figure 6.

4 Boundary Conditions

The same boundary conditions were used as in the GRW model. The king pin was fixed in all directions and the wheels fixed in the vertical direction (z-axis) to simulate the grounded wheels. A single wheel was also fixed in the lateral direction (y-axis) to prevent rigid body motion. For the lateral acceleration (y-axis) load case, all wheels were fixed in the lateral direction (y-axis) to simulate the friction from the grounded wheels.

5 Loads

Unit acceleration loads were applied in the longitudinal direction (x-axis), lateral direction (y-axis) and vertical direction (z-axis) in three separate steps of the analysis.

6 Stress Extraction

A surface stress extrapolation technique was used as described in BS 7608 (2014) to accurately predict the hot spot stress at the tanker band welds. This involved extracting the stresses at distances of 0.4t and t from the weld toe, where t is the shell thickness. The structural stress at the weld toe was then be found by extrapolating the stresses from these two locations.

Four different linear combinations of the unit acceleration loads were considered. These load cases are called the ADR load cases as in the main report.

- Load Case 1: 2g forward acceleration
- Load Case 2: 1g vertical upwards acceleration
- Load Case 3: 2g vertical downwards acceleration
- Load Case 4: 1g lateral sideways acceleration

It was found that Load Case 4 did not result in the most significant stresses amongst the four ADR load cases. For the other three cases, the surface stress extrapolation results are presented as follows: for Load Case 1-3, and for each stress variable (membrane stress, through-wall bending stress and net section stress), the tanker band experiencing the largest tensile stress variable is identified. The stress variable is then plotted around the entire circumference of this band and shown in the figures below.

For Load Case 1 (2g forward acceleration), the results are shown in Figures 7, 8 and 9 for net section stress, membrane stress and through-wall bending stress, respectively. For Load Case 2 (1g vertical upwards acceleration), the results are shown in Figures 10, 11 and 12, and for Load Case 3 (2g vertical downwards acceleration), the results are shown in Figures 13, 14 and 15.

A summary of the key results is shown in Tables 1 and 2. There key findings are as follows:

- The load case resulting in the largest tensile net section stress is ADR Load Case 3 (2g vertical downward acceleration). Tanker band B/10(-) is the location of the largest tensile net section stress at the triple junction where the cradle gusset plate meets the chassis rails and are joined to the tanker shell. At this position (or at both symmetric positions, either side of the tanker axis), the net section stress is 69.46MPa, the through-wall bending stress is 57.93MPa and the membrane stress is 11.53MPa.
- The load case resulting in the largest tensile membrane stress is also ADR Load Case 3 (2g vertical downward acceleration). Tanker band E/10(+) is the location of the largest tensile membrane stress, also at the triple junction where the cradle gusset plate meets the chassis rails and are joined to the tanker shell. At this position (or at both symmetric positions, either side of the tanker axis), the net section stress is 67.45MPa, the through-wall bending stress is 40.53MPa and the membrane stress is 26.92MPa.

By taking into consideration that through-wall bending results in a smaller stress intensity factor than the equivalent magnitude membrane stress, it was decided that the second key finding above would be used to define the most severely stressed location for the ADR load case ECA. That is, even though the total net section stress is smaller (67.45MPa versus 69.46MPa), the degree of bending at the second position is less than the degree of bending at the first position and therefore the overall stress intensity factor will be higher.

7 Conclusions

TWI has produced a detailed finite element model of the J3857 fuel tanker based on the original model provided by GRW. The GRW model represented the global geometry very well. However, TWI made various changes to make the stress prediction more accurate:

1. Potential stress concentrating features were included near the extrusion band weld toes, such as baffle plate holes and undercarriage stiffeners. One bulkhead was corrected to a baffle, as shown in the engineering drawings.
2. The tanker band geometry was adjusted to more accurately represent the bending stiffness of the real band geometry.
3. A more refined mesh was used (2.5 million elements approximately), with quadratic elements in the tanker bands and tanker shell. Local refinement of 5mm elements were also employed around all tanker bands.
4. Hot spot stresses were calculated using the surface stress extrapolation method to more accurately predict stresses at the weld toes, as described in BS 7608 (2014).

The surface stress extrapolation method was used to identify ADR Load Case 3 as generating the most severe stresses.

8 References

BS 7608, 2014: ‘Guide to fatigue design and assessment of steel products’, British Standards Institute.

GRW, 2008 (1): ‘Tank assembly 500 manhole no sensor flanges’, Drawing number: 085-44-500-01, Tanker description: 44100 Lt 6 Comp Tridem.

GRW, 2008 (2): ‘Baffle 2530x1650mm’, Drawing number: A503-27-00, Tanker description: Portfolio drawing.

GRW, 2013: 'Critical crack size & crack growth estimate – an extended study', Product verification and validation report, PVVR20121101, revision no. 3, Danie du Plessis.

Table 1 Severely stressed bands based on net section stress

ADR Load Case	Location of highest net section stress	Net section stress (MPa)	Through-wall bending stress (MPa)	Membrane stress (MPa)
Load Case 1	G/10(-)	58.76	23.02	35.74
Load Case 2	H/10(+)	34.01	19.03	14.98
Load Case 3	B/10(-)	69.46	57.93	11.53

Table 2 Severely stressed bands based on membrane stress

ADR Load Case	Location of highest net section stress	Net section stress (MPa)	Through-wall bending stress (MPa)	Membrane stress (MPa)
Load Case 1	G/10(+)	-3.72	73.22	69.50
Load Case 2	I/10(+)	32.37	-0.99	33.36
Load Case 3	E/10(+)	67.45	40.53	26.92

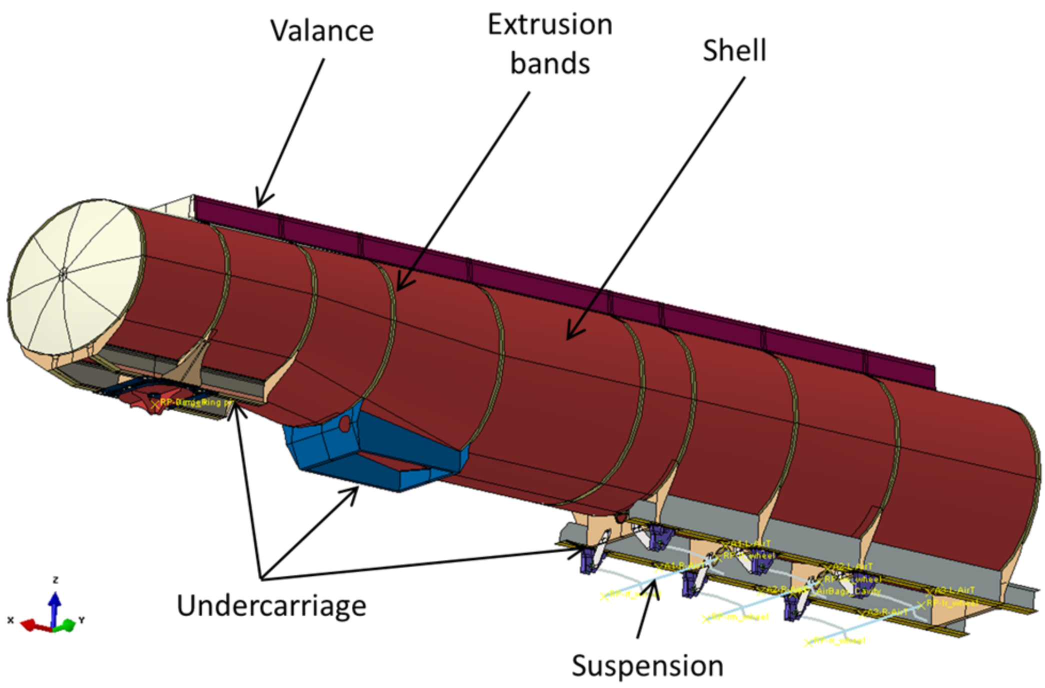

Figure 1 Key features of TWI model geometry.

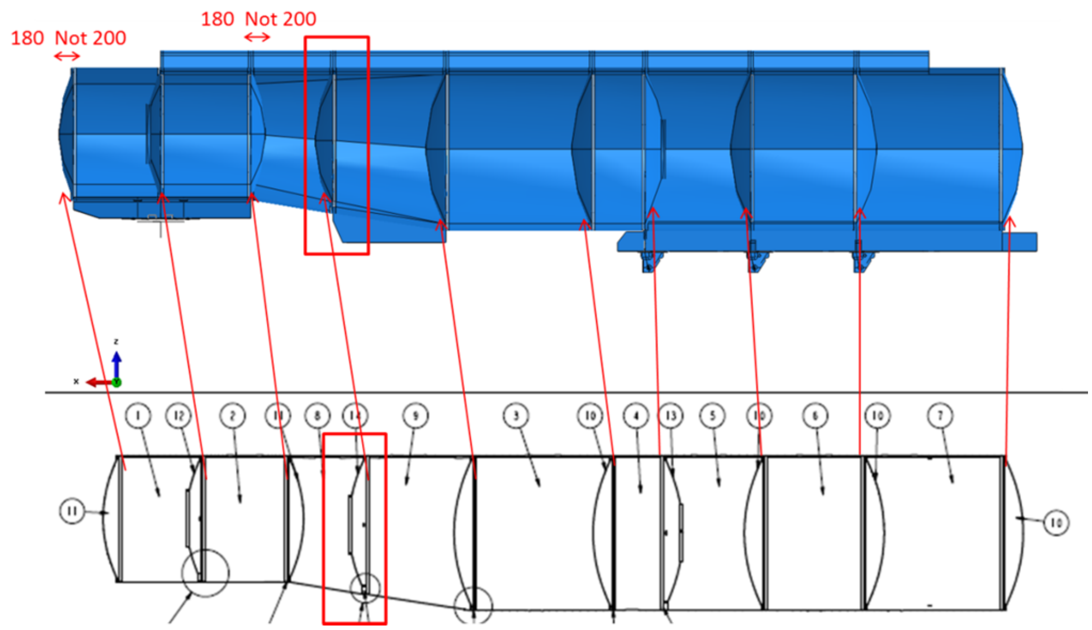

Figure 2 Bulkheads and baffles in GRW model (top) compared to engineering drawings (bottom) (GRW, 2008 (1)).

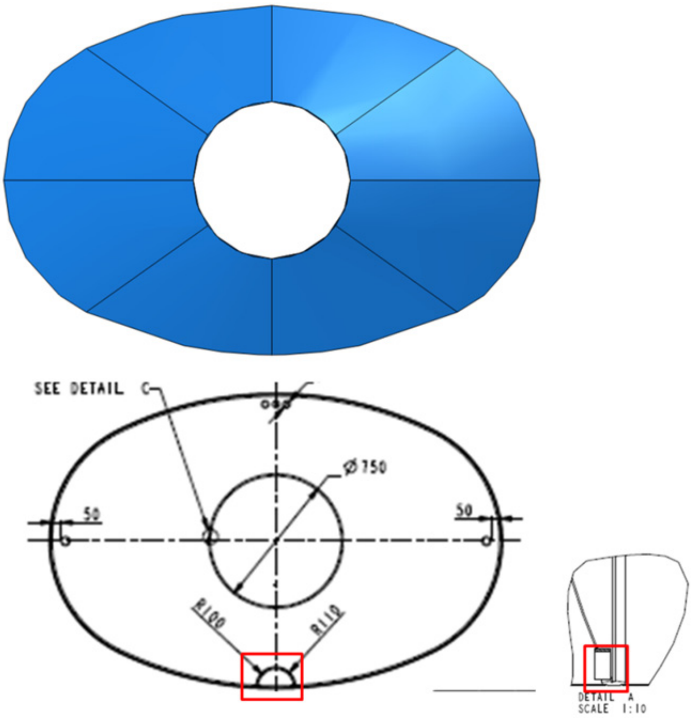

Figure 3 Baffle plate hole detail in model (top) and engineering drawing (bottom) (GRW, 2008 (1), GRW 2008 (2)).

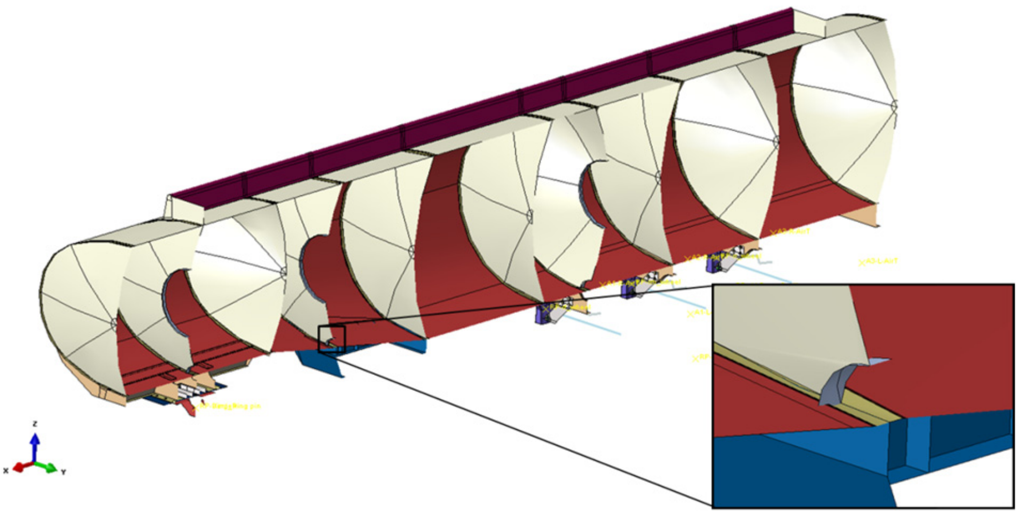

Figure 4 TWI model geometry (only half of model shown to allow view of internal features).

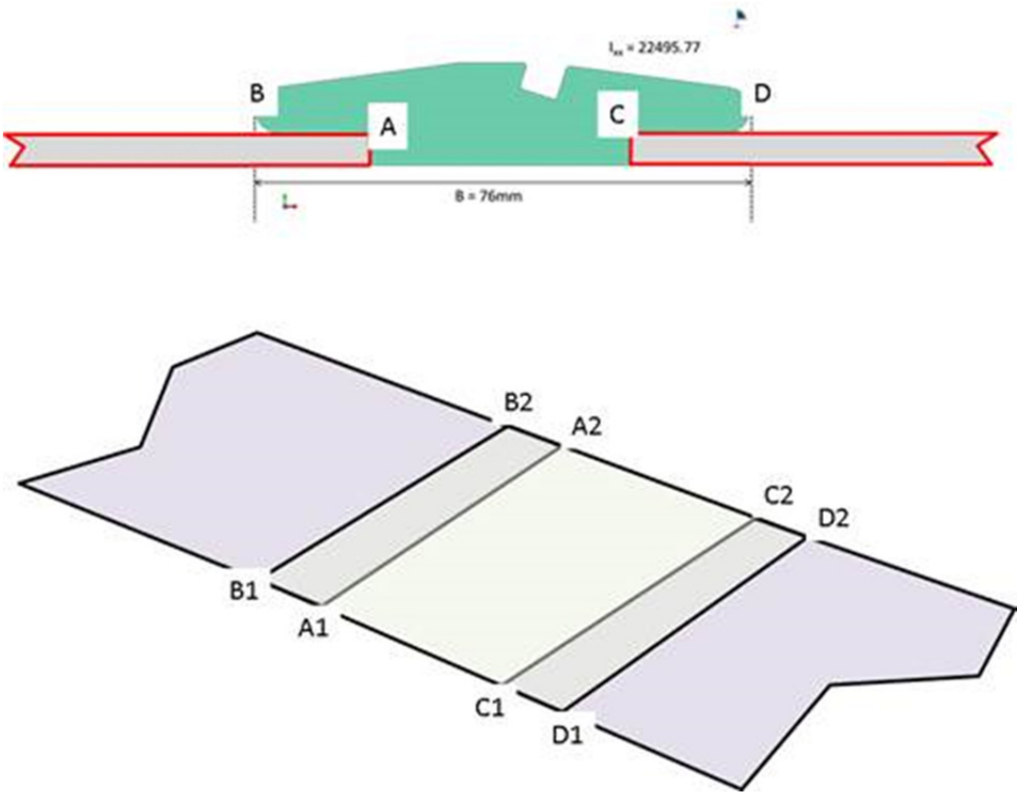

Figure 5 Illustration of model geometry used for tanker bands.

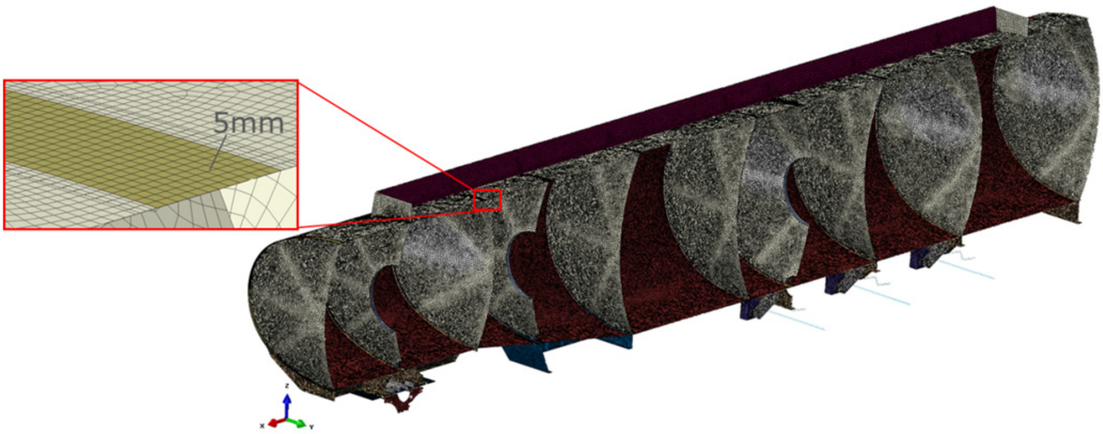

Figure 6 TWI model mesh, with local mesh refinement around all tanker band welds.

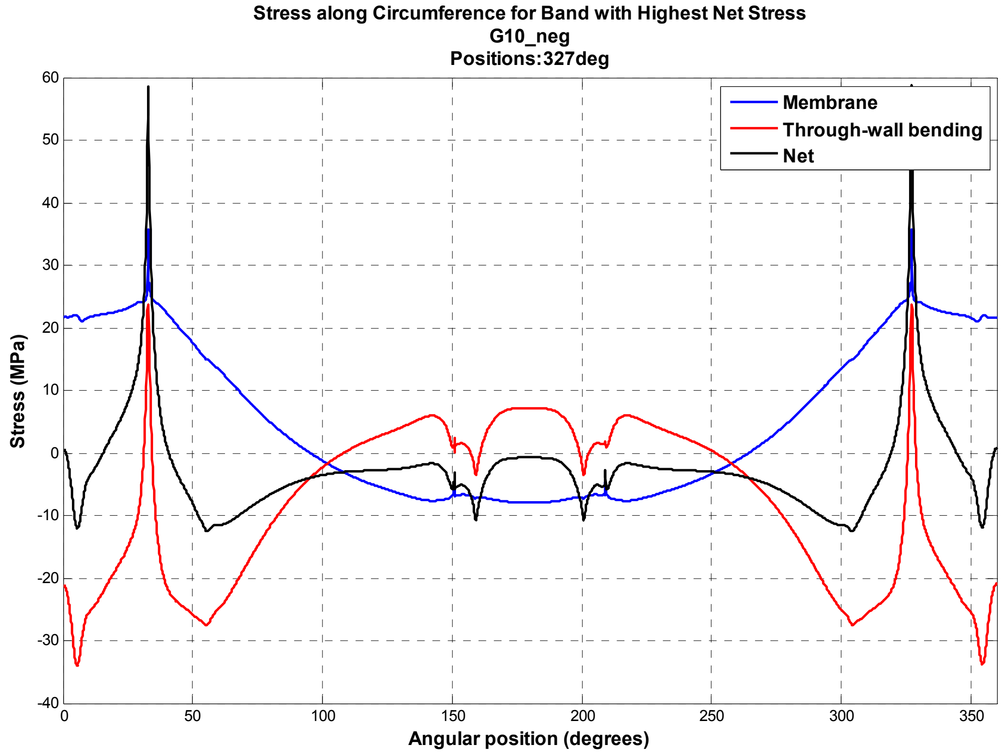

Figure 7 Surface stress extrapolation results for ADR Load Case 1 (2g forwards acceleration) around the circumference for the band where the largest net section stress was extracted.

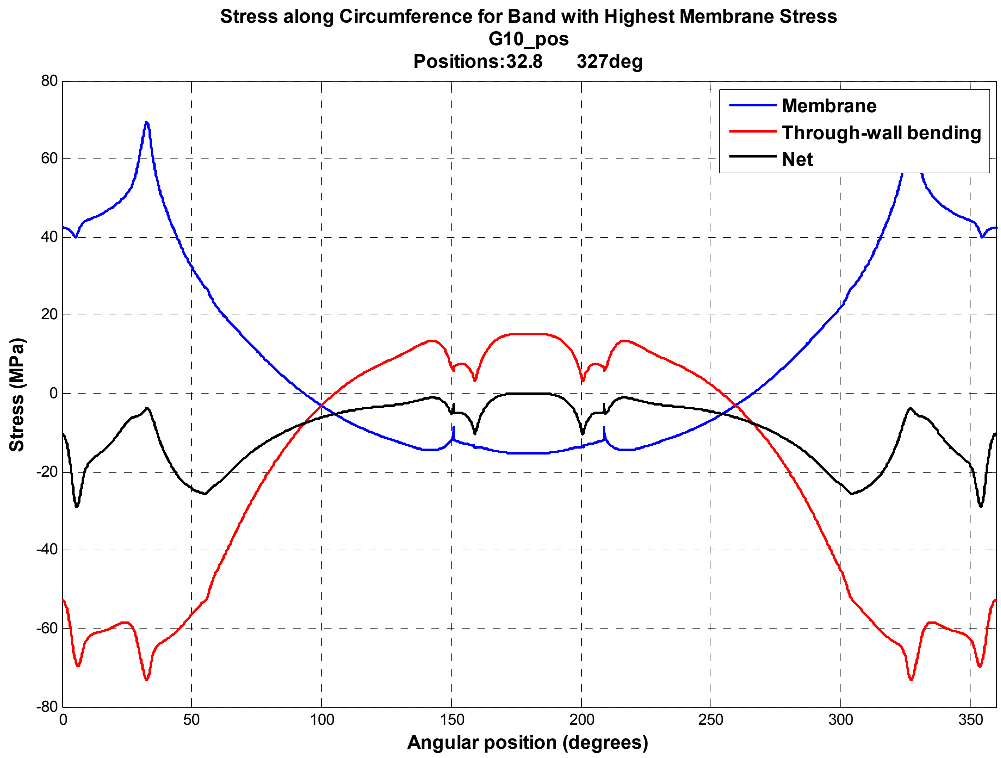

Figure 8 Surface stress extrapolation results for ADR Load Case 1 (2g forwards acceleration) around the circumference for the band where the largest membrane stress was extracted.

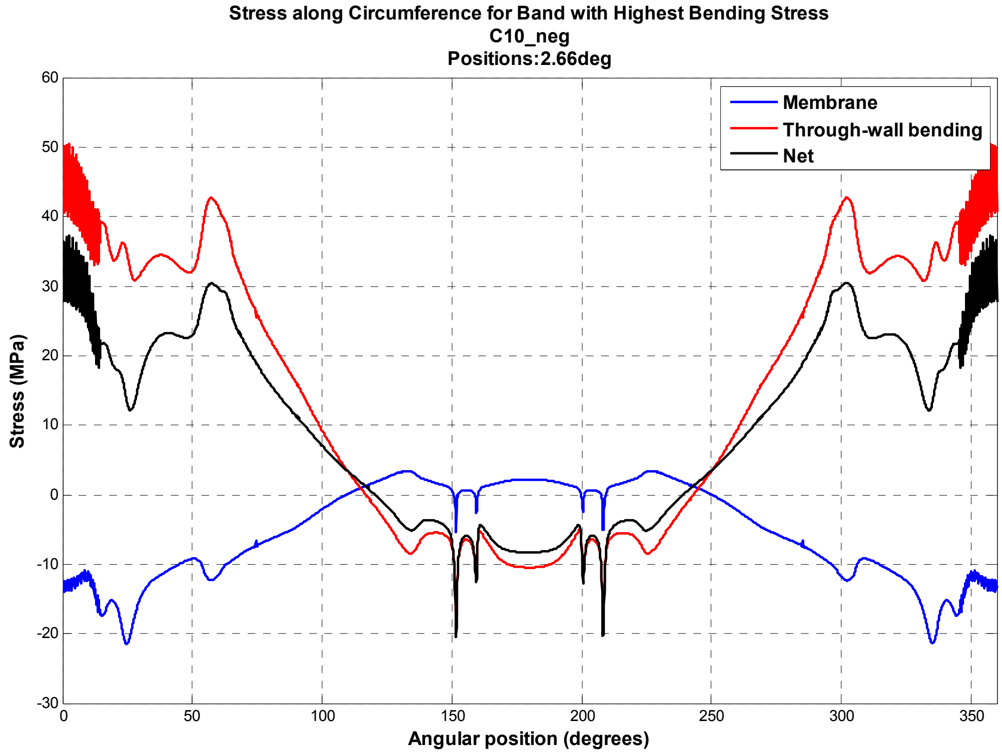

Figure 9 Surface stress extrapolation results for ADR Load Case 1 (2g forwards acceleration) around the circumference for the band where the largest bending stress was extracted.

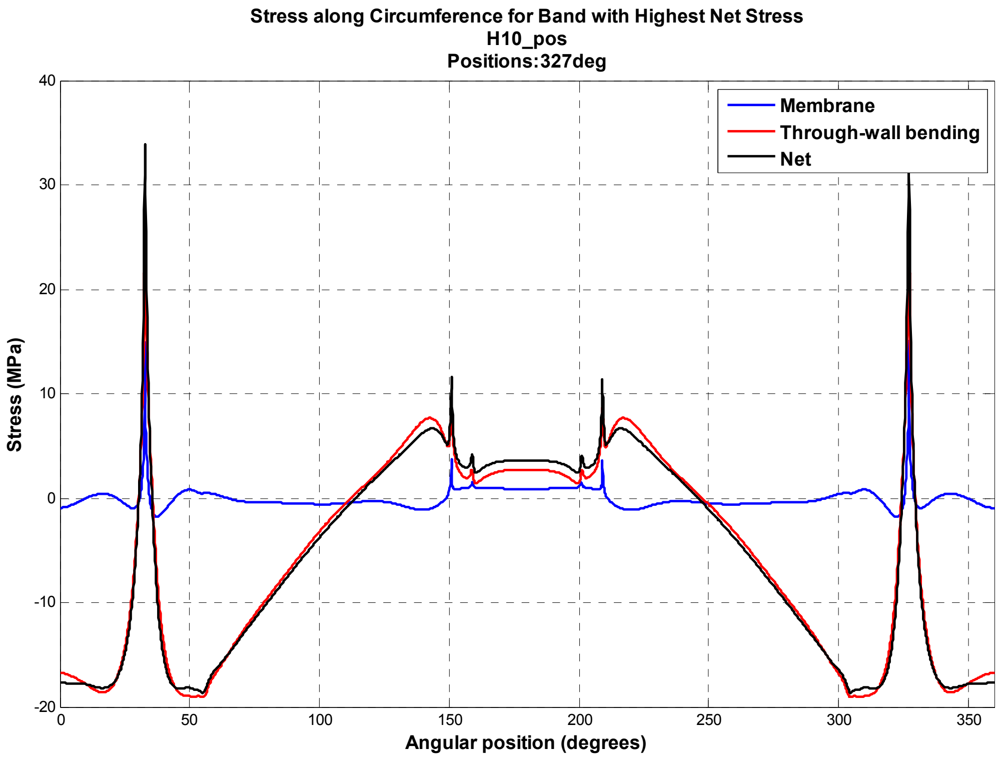

Figure 10 Surface stress extrapolation results for ADR Load Case 2 (1g vertical upwards acceleration) around the circumference for the band where the largest net section stress was extracted.

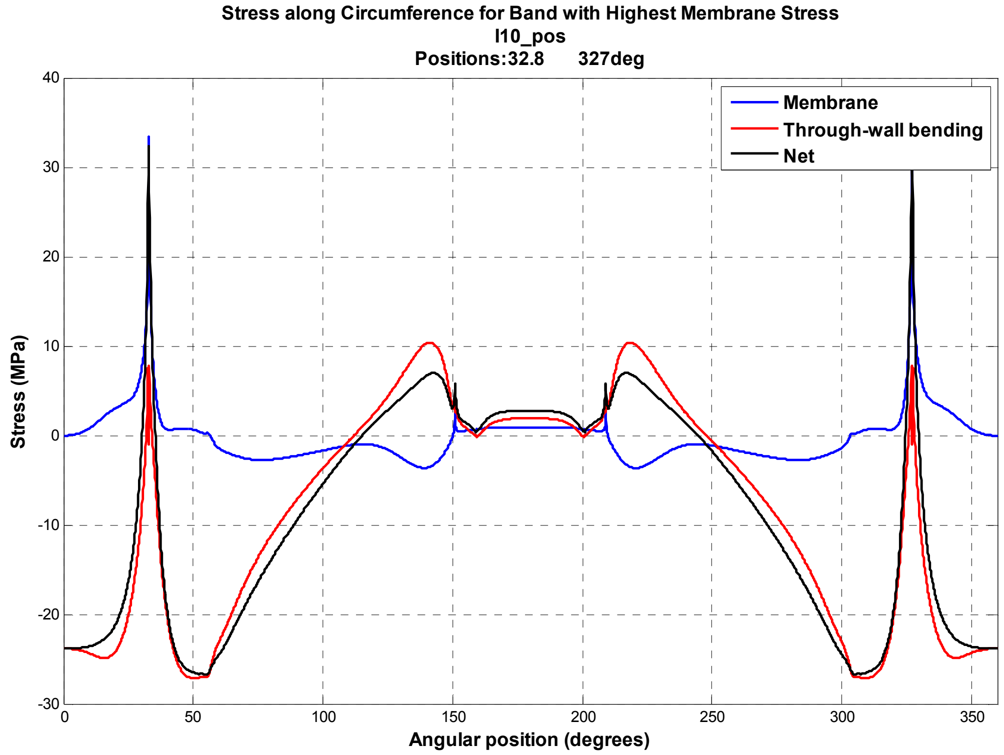

Figure 11 Surface stress extrapolation results for ADR Load Case 2 (1g vertical upwards acceleration) around the circumference for the band where the largest membrane stress was extracted.

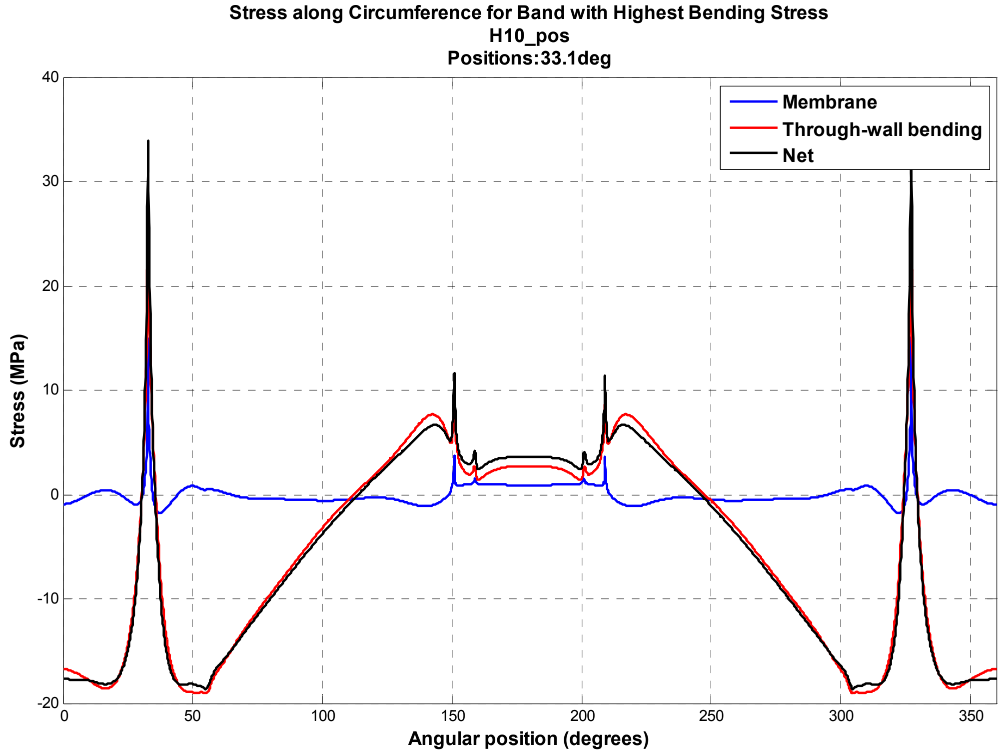

Figure 12 Surface stress extrapolation results for ADR Load Case 2 (1g vertical upwards acceleration) around the circumference for the band where the largest bending stress was extracted.

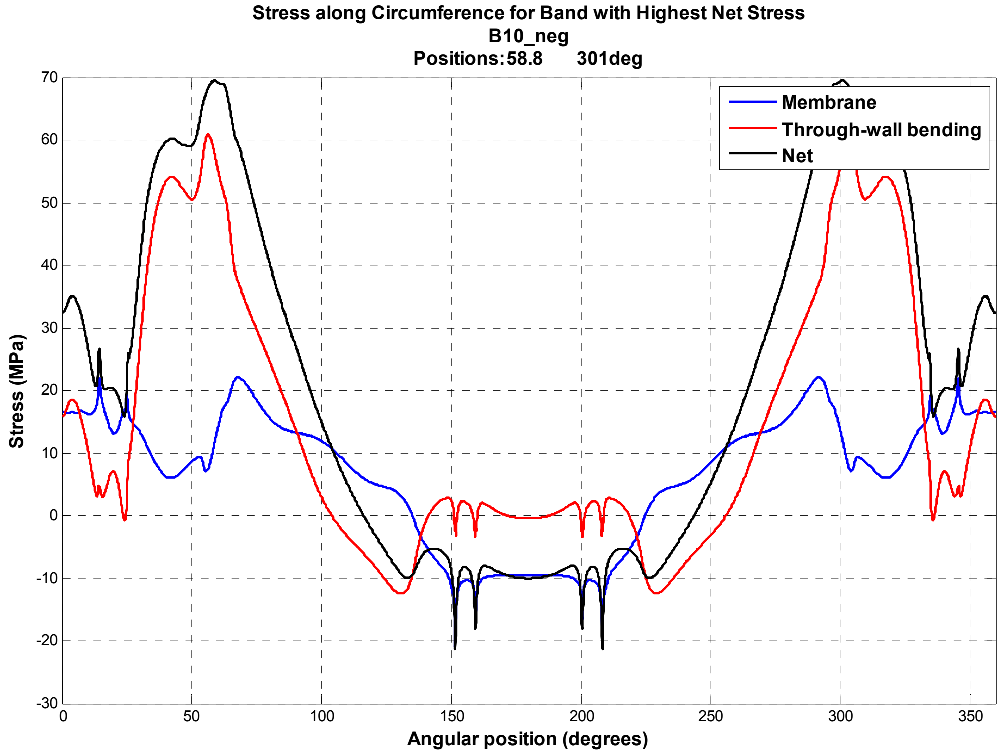

Figure 13 Surface stress extrapolation results for ADR Load Case 3 (2g vertical downwards acceleration) around the circumference for the band where the largest net section stress was extracted.

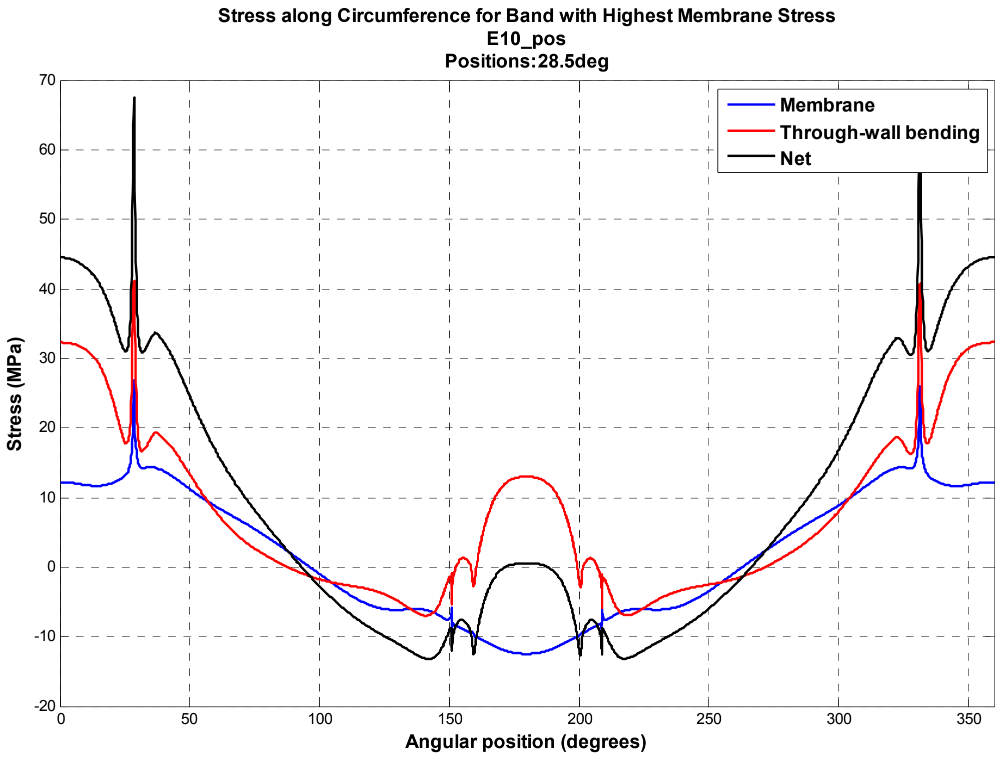

Figure 14 Surface stress extrapolation results for ADR Load Case 3 (2g vertical downwards acceleration) around the circumference for the band where the largest membrane stress was extracted.

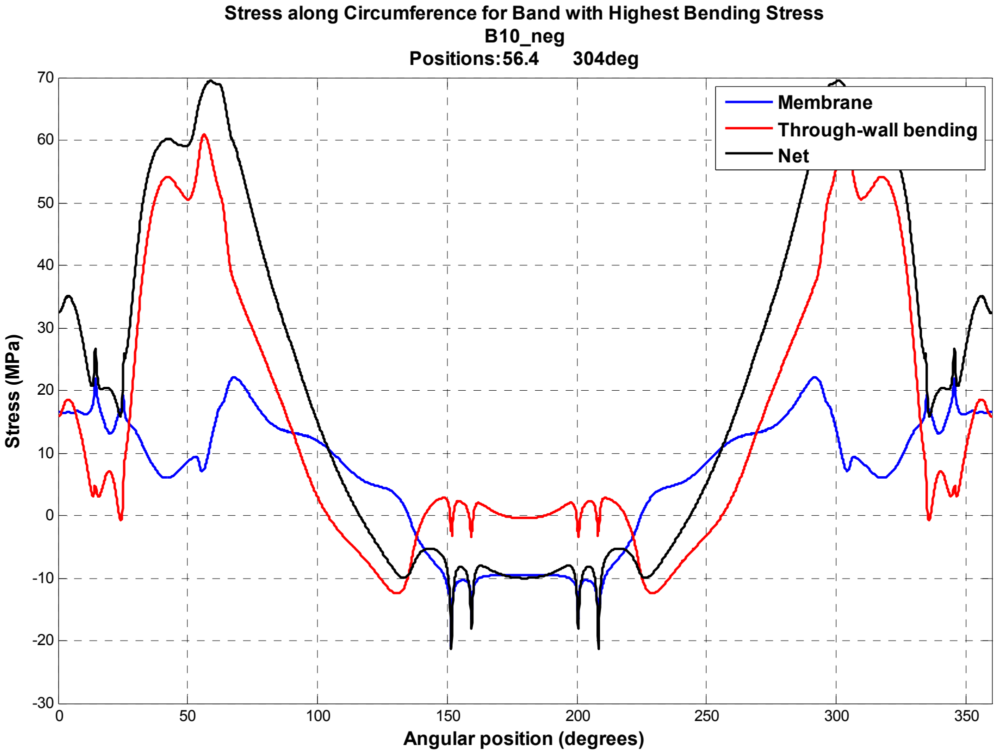

Figure 15 Surface stress extrapolation results for ADR Load Case 3 (2g vertical downwards acceleration) around the circumference for the band where the largest bending stress was extracted.